International Journal of Bifurcation and Chaos, Vol. 19, No. 2 (2009) 665–676

CLUSTER STRUCTURE OF FUNCTIONAL NETWORKS ESTIMATED FROM HIGH-RESOLUTION EEG DATA

ROBERTA SINATRA*
Complex Systems Laboratory,
Scuola Superiore di Catania, Catania, Italy
robertasinatra@gmail.com
rsinatra@ssc.unict.it

FABRIZIO DE VICO FALLANI†
Interdepartmental Research Centre for Models and Information Analysis in Biomedical Systems,
University "La Sapienza", Rome, Italy

LAURA ASTOLFI†,‡, FABIO BABILONI†,‡,
FEBO CINCOTTI† and DONATELLA MATTIA†
†*IRCCS "Fondazione Santa Lucia", Rome, Italy*
‡*Department of Human Physiology and Pharmacology,*
University "La Sapienza", Rome, Italy

VITO LATORA
Department of Physics and Astronomy,
University of Catania,
and INFN Sezione Catania, Italy

Received March 14, 2008; Revised April 9, 2008

We study the topological properties of functional connectivity patterns among cortical areas in the frequency domain. The cortical networks were estimated from high-resolution EEG recordings in a group of spinal cord injured patients and in a group of healthy subjects, during the preparation of a limb movement. We first evaluate global and local efficiency, as indicators of the structural connectivity respectively at a global and local scale. Then, we use the Markov Clustering method to analyze the division of the network into community structures. The results indicate large differences between the injured patients and the healthy subjects. In particular, the networks of spinal cord injured patient exhibited a higher density of efficient clusters. In the Alpha (7–12 Hz) frequency band, the two observed largest communities were mainly composed of the cingulate motor areas with the supplementary motor areas, and of the premotor areas with the right primary motor area of the foot. This functional separation strengthens the hypothesis of a compensative mechanism due to the partial alteration in the primary motor areas because of the effects of the spinal cord injury.

Keywords: Community structure; network efficiency; cortical activity.

*Author for correspondence
The first two authors have contributed equally to the present paper.

1. Introduction

Over the last years, there has been an increasingly large interest in finding significant features from human brain networks. In particular, the concept of functional connectivity plays a central role to understand the organized behavior of anatomical regions in the brain during activity. This organization is thought to be based on the interaction between different specialized areas of cortical sites. Indeed, several methods have been proposed and discussed in the literature, with the aim of estimating the functional relationships among the physiological signals [David *et al.*, 2004; Lee *et al.*, 2003] obtained from different neuro-imaging devices such as the functional Magnetic Resonance Imaging (fMRI) scanner, electroencephalography (EEG) and magnetoencephalography (MEG) apparatus [Horwitz, 2003]. Recently, a multivariate spectral technique called Directed Transfer Function (DTF) has been proposed [Kaminski *et al.*, 2001] to determine directional influences between any given pair of channels in a multivariate data set. This estimator is able to characterize at the same time direction and spectral properties of the brain signals, requiring only one multivariate autoregressive (MVAR) model to be estimated from all the EEG channel recordings. The DTF index has been demonstrated [Kaminski *et al.*, 2001] to rely on the key concept of Granger causality between time series — an observed time series $x(n)$ leads to another series $y(n)$ if the knowledge of past $x(n)$s significantly improves the prediction of $y(n)$ — [Granger, 1969]. However, the extraction of salient characteristics from brain connectivity patterns is an openly challenging topic, since often the estimated cerebral networks have a relative large size and complex structure. Consequently, there is a wide interest in the development of mathematical tools that could describe in a concise way the structure of the estimated cerebral networks [Tononi *et al.*, 1994; Stam, 2004; Salvador, 2005; Sporns, 2002].

Functional connectivity networks estimated from EEG or magnetoencephalographic (MEG) recordings can be analyzed with tools that have been already proposed for the treatments of complex networks as graphs [Strogatz, 2001; Wang & Chen, 2003; Sporns *et al.*, 2004; Stam *et al.*, 2006a]. Such an approach can be useful, since the use of mathematical measures summarizing graph properties allows for the generation and the testing of particular hypothesis on the physiologic nature of the functional networks estimated from high-resolution EEG recordings. However, first results have been obtained for a set of anatomical brain networks [Strogatz, 2001; Sporns *et al.*, 2002]. In these studies, the authors have employed two characteristic measures, the *average shortest path* L and *the clustering index* C, to extract respectively the global and local properties of the network structure [Watts & Strogatz, 1998]. They have found that anatomical brain networks exhibit many local connections (i.e. a high C) and a shortest separation distance between two randomly chosen nodes (i.e. a low L). Hence, anatomical brain networks have been designated as small-world in analogy with the concept of the small-world phenomenon observed more than 30 years ago in social systems [Milgram, 1967].

Many types of functional brain networks have been analyzed in a similar way. Several studies based on different imaging techniques like fMRI [Salvador *et al.*, 2005; Eguiluz *et al.*, 2005; Achard & Bullmore, 2007], MEG [Stam *et al.*, 2006a, 2006b; Bassett *et al.*, 2006; Bartolomei *et al.*, 2006] and EEG [Micheloyannis *et al.*, 2006; Stam *et al.*, 2007] have shown that the estimated functional networks can indeed exhibit the small-world property. In the functional brain connectivity context, these properties have been demonstrated to reflect an optimal architecture for the information processing and propagation among the involved cerebral structures [Lago-Fernandez *et al.*, 2000; Sporns *et al.*, 2000]. In particular, a high *clustering index* C is an indication of the presence in the network of a large number of triangles. However, this index alone does not return detailed information on the presence of larger connected clusters of nodes. This fact makes up a real obstacle in the analysis of the network properties especially in the field of the Neuroscience where the correlated behavior of different cortical regions plays a fundamental role in the correct understanding of cerebral systems. Methods to detect the community structures in a graph, i.e. tightly connected group of nodes, are now available in the market [Harary & Palmer, 1973]. Communities (or clusters or modules) are groups of vertices that probably share common properties and/or play similar roles within the graph [Boccaletti *et al.*, 2006]. Hence, communities may correspond to groups of pages of the World Wide Web dealing with related topics [Flake *et al.*, 2002], to functional modules such as cycles and pathways in metabolic networks [Guimer & Amaral, 2005; Palla *et al.*, 2005], to groups of

affine individuals in social networks [Girvan & Newman, 2002; Lusseau & Newman, 2004], to compartments in food webs [Pimm, 1979; Krause *et al.*, 2003] and so on. Finding the communities within a cerebral network allows identifying the hierarchy of functional connections within a complex architecture. This opportunity would represent an interesting way to improve the basic understanding of the brain functioning. Indeed, some cortical regions are supposed to share a large number of functional relationships during the performance of several motor and cognitive tasks. This characteristic leads to the formation of highly connected clusters within the brain network. These functional groups consist of a certain number of different cerebral areas that are cooperating more intensively in order to complete a task successfully.

In the present paper, we focus on a study of the structural properties of functional networks estimated from high-resolution EEG signals in a group of spinal cord injured patients during the preparation of a limb movement. In particular, we first investigate some indicators of the connectivity at a global and local scale. Then we analyze the networks by studying their structure in communities, and we compare the results with those obtained from a group of healthy subjects.

2. Methods

2.1. *High-resolution EEG recordings in SCI patients and healthy subjects*

All the experimental subjects participating in the study were recruited by advertisement. Informed consent was obtained for each subject after the explanation of the study, which was approved by the local institutional ethics committee. The spinal cord injured (SCI) group consisted of five patients (age 22–25 years; two females and three males). Spinal cord injuries were of traumatic aetiology and located at the cervical level (C6 in three cases, C5 and C7 in two cases, respectively); patients had not suffered from a head or brain lesion associated with the trauma leading to the injury. The control (CTRL) group consisted of five healthy volunteers (age 26–32 years; five males). They had no personal history of neurological or psychiatric disorder; they were not taking medication, and were not abusing alcohol or illicit drugs. For EEG data acquisition, subjects were comfortably seated on a reclining chair, in an electrically shielded, dimly lit room. They were asked to perform a brisk protrusion of their lips (lip pursing) while they were performing (healthy subjects) or attempting (SCI patients) a right foot movement. The choice of this joint movement was suggested by the possibility to trigger the SCIs attempt of foot movement. In fact, patients were not able to move their limbs; however they could move their lips. By attempting a foot movement associated with a lips protrusion, they provided an evident trigger after the volitional movement activity. This trigger was recorded to synchronize the period of analysis for both the considered populations. The task was repeated every 6–7 seconds, in a self-paced manner, and the 100 single trials recorded will be used for the estimate of functional connectivity by means of the Directed Transfer Function (DTF, see following paragraph). A 96-channel system (BrainAmp, Brainproducts GmbH, Germany) was used to record EEG and EMG electrical potentials by means of an electrode cap and surface electrodes, respectively. The electrode cap was built accordingly to an extension of the 10–20 international system to 64 channels. Structural MRIs of the subjects head were taken with a Siemens 1.5T Vision Magnetom MR system (Germany).

2.2. *Cortical activity and functional connectivity estimation*

Cortical activity from high-resolution EEG recordings was estimated by using realistic head models and cortical surface models with an average of 5.000 dipoles, uniformly disposed. Estimation of the current density strength, for each one of the 5.000 dipoles, was obtained by solving the Linear Inverse problem, according to techniques described in previous papers [Babiloni *et al.*, 2005; Astolfi *et al.*, 2006]. By using the passage through the Tailairach coordinates system, twelve Regions Of Interest (ROIs) were then obtained by segmentation of the Brodmann areas on the accurate cortical model utilized for each subject. The ROIs considered for the left (_L) and right (_R) hemispheres are: the primary motor areas for foot (MF_L and MF_R) and lip movement (ML_L and ML_R); the proper supplementary motor area (SM_L and SM_R); the standard premotor area (6_L and 6_R); the cingulated motor area (CM_L and CM_R) and the associative Brodmann area 7 (7_L and 7_R). For each EEG time point, the magnitude of the five thousand dipoles composing the cortical model was estimated

by solving the associated Linear Inverse problem [Grave de Peralta & Gonzalez Andino, 1999]. Then, the average activity of dipoles within each ROI was computed. In order to study the preparation to an intended foot movement, a time segment of 1.5 seconds before the lips pursing was analyzed; lips movement was detected by means of an EMG. The resulting cortical waveforms, one for each predefined ROI, were then simultaneously processed for the estimation of functional connectivity by using the Directed Transfer Function. The DTF is a full multivariate spectral measure used to determine the directed influences between any given pair of signals in a multivariate data set [Kaminski *et al.*, 2001]. In order to be able to compare the results obtained for data entries with different power spectra, the normalized DTF was adopted. It expresses the ratio of influence of element j to element i with respect to the influence of all the other elements on i. Details on the DTF equations in the treatment of EEG signals have been largely described in previous papers [Astolfi *et al.*, 2005; Babiloni *et al.*, 2005]. In the present study, we selected four frequency bands of interest (Theta 4–7 Hz, Alpha 8–12 Hz, Beta 13–29 Hz and Gamma 30–40 Hz) and we gathered the respective cortical networks by averaging the values within the respective range. In order to consider only the functional links that are not due to chance, we adopted a Monte Carlo procedure. In particular, we contrasted each DTF value with a surrogate distribution of one thousand DTF values obtained by shuffling the signal samples in the original EEG data set. Then, we considered a threshold value by computing the 99th percentile of the distribution and we filtered the original DTF values by removing the edges with intensity below the statistical threshold.

2.3. *Evaluation of global and local efficiency*

A graph is an abstract representation of a network. A graph G consists of a set of vertices (or nodes) $\mathscr{V}$ and a set of edges (or connections) $\mathscr{L}$ indicating the presence of some sort of interaction between the vertices. A graph can be described in terms of the so-called adjacency matrix A, a square matrix such that, when a weighted and directed edge exists from the node i to j, the corresponding entry of the adjacency matrix is $A_{ij} \neq 0$; otherwise, $A_{ij} = 0$. Two measures are frequently used to characterize the local and global structure of unweighted graphs: the average shortest path L and the clustering index C [Watts & Strogatz, 1998; Newman, 2003; Grigorov, 2005]. The former measures the average distance between two nodes, the latter indicates the tendency of the network to form highly connected clusters of nodes. Recently, a more general setup has been proposed to study weighted (also unconnected) networks related to efficiency [Latora & Marchiori, 2001, 2003]. The efficiency e_{ij} in the communication between two nodes i and j is defined as the inverse of the shortest distance between the vertices. Note that in weighted graphs the shortest path is not necessarily the path with the smallest number of edges. In the case when the two nodes are not connected, the distance is infinite and $e_{ij} = 0$. The average of all the pair-wise efficiencies e_{ij} is the global-efficiency E_g of the graph G:

$$E_g(G) = \frac{1}{N(N-1)} \sum_{i \neq j \in \mathscr{V}} \frac{1}{d_{ij}} \tag{1}$$

where N is the number of vertices composing the graph. The local properties of the graph can be characterized by evaluating for every vertex i the efficiency of G_i, which is the subgraph induced by the neighbors of the node i [Latora & Marchiori, 2001]. Thus, we defined the local-efficiency E_l of graph G as the average:

$$E_l(G) = \frac{1}{N} \sum_i E_g(G_i). \tag{2}$$

Since node i does not belong to subgraph G_i, the local efficiency measures how the communication among the first neighbors of i is affected by the removal of i [Latora & Marchiori, 2005, 2007]. Hence, the local efficiency is an indicator of the level of fault-tolerance of the system. Separate ANOVAs were conduced for each of the two variables E_g and E_l. Statistical significance was fixed at 0.05, and main factors of the ANOVAs were the "between" factor GROUP (with two levels: SCI and CTRL) and the "within" factor BAND (with four levels: Theta, Alpha, Beta and Gamma). Greenhouse & Geisser correction has been used for the protection against the violation of the sphericity assumption in the repeated measure ANOVA. Besides post-hoc analysis with the Duncan's test and significance level at 0.05 has been performed.

2.4. *Detection of community structures*

In order to detect the community structures, we have implemented the Markov Clustering (MCl)

algorithm [Vandongen, 2000; Enright *et al.*, 2002]. It is one algorithm of a few available that works even with directed graphs and it is based on the properties of the dynamical evolution of random walkers moving on the graph. This approach is also useful since it manages to achieve reliable results when the graph contains self-loops, i.e. edges connecting a node to itself. Since a community is a group of densely connected nodes, a random walker that started in a node of a given community will leave this cluster only after having visited a large number of the community's nodes. Hence, the basic idea implemented in the algorithm is to favor the random motion within nodes of the same community. This is obtained by alternating the application of two operators on the transition matrix of the random walk: the expansion operator and the inflation one. The expansion operator applied on a given matrix returns its square power, while the inflation operator corresponds to the Hadamard power of the same matrix, followed by a scaling step. In practice, the algorithm works as follows:

1. Take the adjacency matrix A and add a self-loop to each node, i.e. set $A_{ii} = 1$ for $i = 1, 2, \ldots, N$;
2. Obtain from A the transition probability matrix W that describes the random motion: $W_{ij} = A_{ij}/\sum_k A_{kj}$. Every element W_{ij} expresses the probability to go from j to i in one step. W is a stochastic matrix i.e. a matrix of non-negative elements and where the sum of elements of each column is normalized to one: $\sum_{i=1}^{N} W_{ij} = 1$;
3. Take the square of W (expansion step);
4. Take the r$^{\text{th}}$ power ($r > 1$) of every element of W^2 and normalize each column to one to obtain a new stochastic matrix W': $W' = [(W^2)_{ij}]^r / (\sum_k [(W^2)_{kj}]^r)$ (inflation step);
5. Go back to step 3.

Step 3 corresponds to computing random walks of "higher-lengths", that is to say random walks with many steps. Step 4 will serve to enhance the elements of a column having higher values. This means, in practice, that the most probable transition from node j will become even more probable compared to the other possible transitions from node j. The algorithm converges to a matrix invariant under the action of expansion and inflation. The graph associated to such matrix consists of different star-like components; each of them constitutes a community (or cluster) and its central node can be interpreted as the basin of attraction of the community. For a given $r > 0$, MCl always converges to the same matrix; for this reason it is classified as a parametric and deterministic algorithm. The parameter r tunes the granularity of the clustering, meaning that a small r corresponds to a few big clusters, while a big r returns smaller clusters. In the limit of $r \to 1$ only one cluster is detected. In the present study, an analysis at different levels of granularity has been performed in order to find the value of r which better fits with the experimental data. Then we have represented how the average of the number of clusters changes as a function of r (Fig. 3). Finally the value $r = 1.5$ has been chosen to study in detail how the nodes are organized in clusters.

3. Results

Figure 1 shows the realistic head model obtained for a representative subject. The twelve ROIs used in the present study are illustrated in color on the cortex model that is gray colored. At the bottom of Fig. 1, we report the adjacency matrices representing the cortical networks estimated, in the Alpha frequency band, from the two analyzed populations during the movement preparation. Note that such networks are directed. Consequently, the obtained adjacency matrix is not symmetric. The level of gray within each matrix in figure encodes the number of subjects that hold the functional connection identified by row i and column j.

As a measure of global and local performances of the network structure we have evaluated the global-efficiency E_g and the local-efficiency E_l indices obtained for each frequency band and for each subject. The average values of E_g and E_l derived from the healthy group (CTRL) and from the group of patients (SCI) are illustrated for each band in the scatter plot in Fig. 2. We have performed an Analysis of Variance (ANOVA) of the obtained results. The E_g variable showed no significant differences for the main factors GROUP and BAND. In particular, the "between" factor GROUP was found having an F value of 0.83, $p = 0.392$ while the "within" factor BAND showed an F value of 0.002 and $p = 0.99$. The ANOVA performed on the E_l variable revealed a strong influence of the between factor GROUP ($F = 32.67$, $p = 0.00045$); while the BAND factor and the interaction between GROUP X BAND was found not significant ($F = 0.21$ and $F = 0.91$, respectively, p values equal to 0.891 and 0.457). Post-hoc tests revealed a significant difference between the two

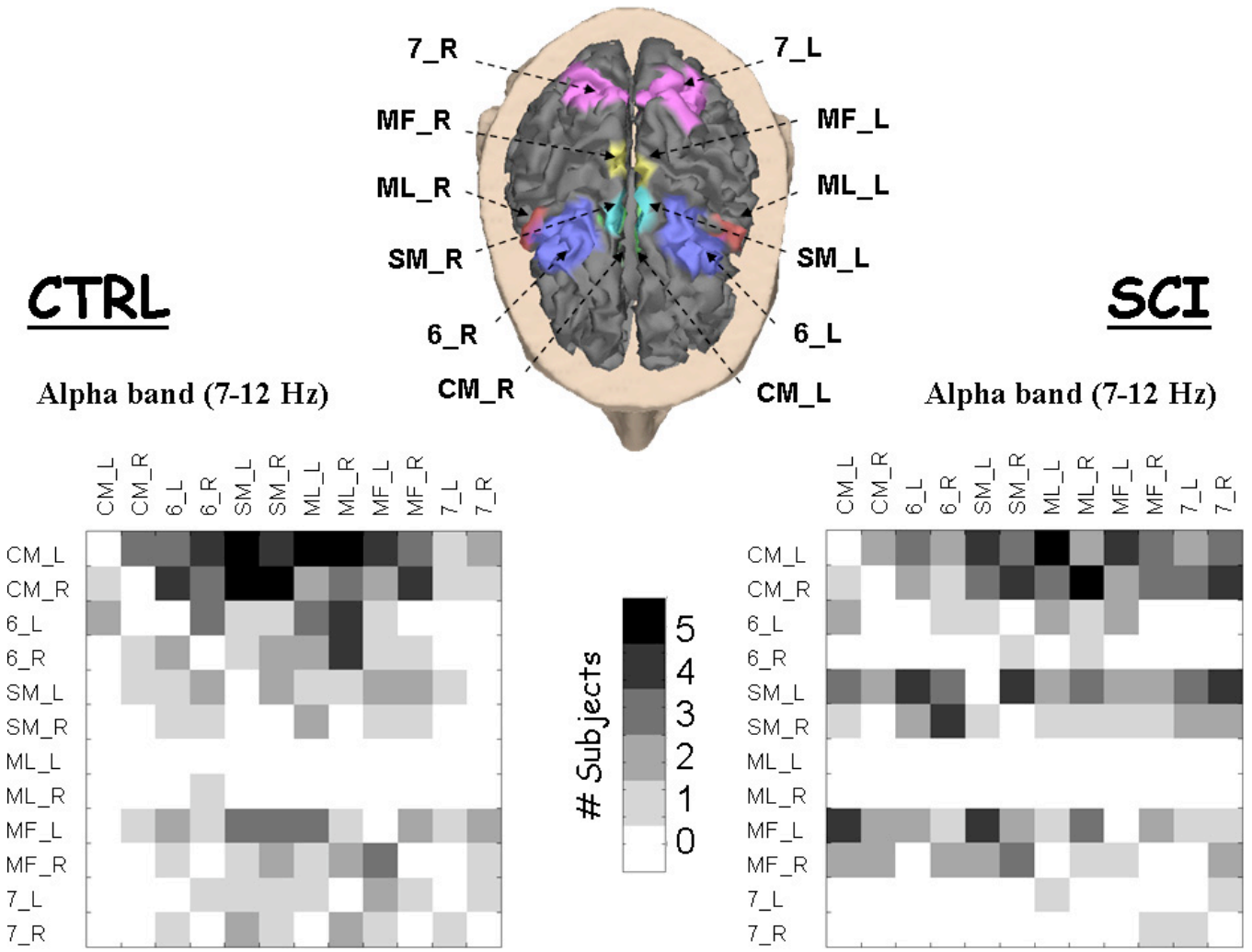

Fig. 1. (Top) Reconstruction of the head model from magnetic resonance images. The twelve regions of interest (ROIs) are illustrated in color on the gray cortex and labeled according to previously defined acronyms. (Bottom left) Adjaceny matrix for the control group (CTRL) in the Alpha (7–12 Hz) band. The level of gray encodes the number of subjects that hold the functional connection identified by the row i and column j. (Bottom right) Adjacency matrix for the patients group (SCI) in the Alpha band. Same conventions as above.

examined experimental groups (SCI, CTRL) in the Alpha and Beta band ($p = 0.01, 0.03$, respectively). In particular, the average local-efficiency of the SCI networks was significantly higher than the CTRL networks for all these bands.

The identification of functional clusters within the cortical networks estimated in the control subjects and in the spinal cord injured patients during the movement preparation was addressed through the MCl algorithm (see Methods — Detection of Community Structures (2.4)). In Fig. 3 the average number of clusters detected in the CTRL and SCI networks is reported as a function of the granularity parameter r. As it can be observed, for every value of r, and for both the Alpha and Beta bands, the average number of clusters is greater for the SCI group than for the CTRL one. One of the main problems with the MCl algorithm is the choice of the value of the granularity parameter to be used. Usually good values of r are in the range $]1, 3[$ [Vandongen, 2000; Enright *et al.*, 2002]. For the case under study here, the presence of a plateau in Fig. 3 indicates that there is a region of values such that the number of clusters does not strongly depend on r. We have decided to adopt the granularity $r = 1.5$ that is a value in the plateau. For this value of r, the average number of clusters in the Alpha band is equal to 3.2 for the cortical networks of the control subjects, while it is equal to 5 for the spinal cord injured patients. In the Beta band, the average

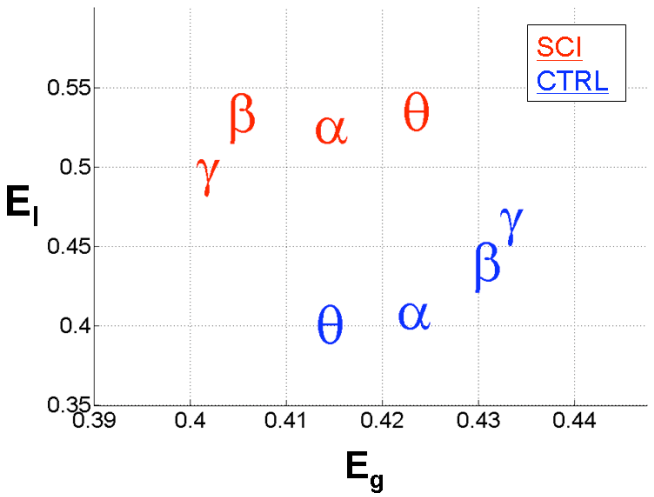

Fig. 2. Scatter plot of the average efficiency indexes obtained from the estimated cortical networks. Global-efficiency is on the x-axis; local-efficiency is on the y-axis. The Greek symbol encodes the frequency band (θ Theta, α Alpha, β Beta and γ Gamma) and it represents the average of the values computed from the control (CTRL, blue-colored font) and spinal cord injured group (SCI, red-colored font).

number of cluster is 3.4 for the CTRL networks and 4.6 for the SCI networks, as can be observed at the bottom in Fig. 3.

Figure 4 illustrates the partitioning of the cortical networks estimated in the Alpha band for a representative subject of the control (CTRL) group and for a representative patient of the spinal cord injured (SCI) group.

Functional networks are represented as three-dimensional graphs on the realistic head model of the experimental subjects. The color of each node, located in correspondence to each cortical area (ROI), encodes the cluster to which the node belongs. The functional clusters detected within the cortical networks in all the subjects and patients participating in the present study are listed in the following tables. Table 1 presents the results obtained in the Alpha band while Table 2 presents the results obtained in the Beta band.

In the Alpha band, the CTRL networks do not present a particularly complicated division into clusters, since for each subject the large part of the cortical areas belong to a unique large community (Cluster 1). In general, the SCI networks organized in a larger number of clusters are more clustered, and two main communities can be observed (Clusters 1 and 2). The first community is mostly composed of the cingulate motor areas (CM_L and CM_R), the supplementary motor areas (SM_L and SM_R) and the left primary motor area (MF_L). The second community is predominantly composed of the left premotor areas (6_L) and the right primary motor area of the foot (MF_R). The remaining ROIs tend to form isolated groups.

In the Beta band both the cortical networks of the control and spinal cord injured group tend to get organized in two main modules (Clusters 1 and 2). In particular, while for both the populations the first cluster is principally composed of the cingulate

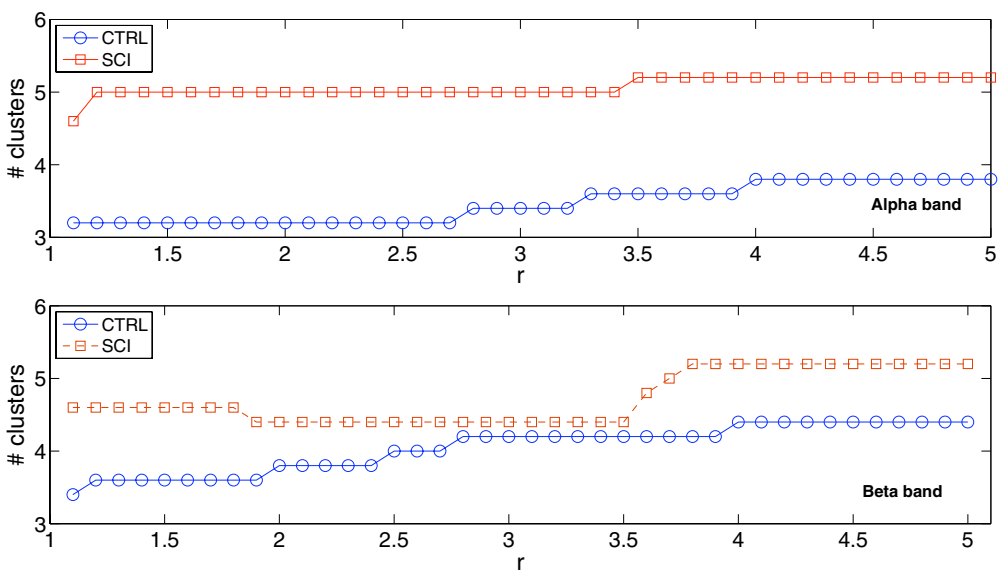

Fig. 3. Representation of the mean number of clusters for CTRL (blue circles) and SCI (red squares) groups as a function of r, granularity parameter of the MCl algorithm, in both the Alpha (top) and Beta bands (bottom).

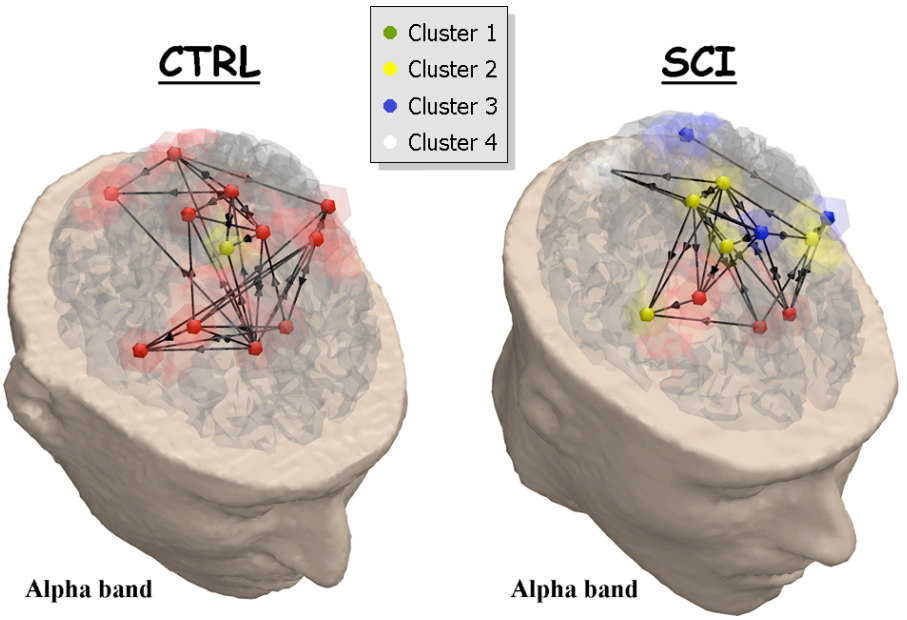

Fig. 4. Graphical representation of the identified clusters of ROIs within the functional networks estimated from a representative control (CTRL) subject and spinal cord injured (SCI) patient during the movement preparation in the Alpha band. The functional network is illustrated as a three-dimensional graph on the realistic cortex model. Spheres located at the barycenter of each ROI represent nodes. Black directed arrows represent edges. The graph partitioning is illustrated through the nodes coloring. Nodes with same colors belong to the same cluster.

Table 1. Cortical network partitioning in the Alpha frequency band.

	CTRL					
	Cluster 1	Cluster 2	Cluster 3	Cluster 4	Cluster 5	Cluster 6
ALFA	CM_L,CM_R,6_L,6_R, SM_L,ML_L,ML_R,MF_L, MF_R,7_L,7_R	SM_R	0	0	0	0
ARGI	CM_L,CM_R,6_L,6_R, ML_R,MF_L,MF_R,7_L, 7_R	SM_L	SM_R	ML_L	0	0
CIFE	CM_L,CM_R,6_L,6_R, SM_L,SM_R,ML_R,MF_L, MF_R,7_R	ML_L	7_L	0	0	0
MADA	CM_L,CM_R,6_L,SM_R, ML_L,7_L,7_R	6_R,SM_L,ML_R, MF_L,MF_R	0	0	0	0
MAMA	CM_L,CM_R,6_L,6_R, SM_L,SM_R,ML_L, MF_L,MF_R	ML_R	7_L	7_R	0	0
	SCI					
	Cluster 1	Cluster 2	Cluster 3	Cluster 4	Cluster 5	Cluster 6
BARO	CM_L,CM_R,6_R	6_L,SM_R, ML_R,MF_L,MF_R	SM_L,ML_L, 7_L	7_R	0	0
IRIO	CM_L,CM_R,SM_L, SM_R,ML_R,MF_L,7_L	6_L	6_R	ML_L	MF_R	7_R
MASI	CM_L,CM_R,6_L,SM_L, SM_R,ML_L,ML_R,MF_L	6_R,MF_R,7_R	7_L	0	0	0
POAL	CM_L,CM_R,6_R,SM_R	6_L, SM_L, MF_R,7_L	ML_L	ML_R	MF_L	7_R
TRDA	CM_L,CM_R,SM_L,SM_R, ML_L,MF_L,MF_R	6_L	6_R	ML_R	7_L	7_R

Table 2. Cortical network partitioning in the Beta frequency band.

	CTRL				
	Cluster 1	Cluster 2	Cluster 3	Cluster 4	Cluster 5
ALFA	CM_L,CM_R,6_L,6_R, SM_L,SM_R,ML_L,ML_R, MF_L,MF_R	7_L	7_R	0	0
ARGI	CM_L,CM_R,6_R,ML_L, ML_R,MF_L,7_L	6_L,SM_L,MF_R	SM_R	7_R	0
CIFE	CM_L,CM_R,6_L,SM_L, SM_R,ML_L,MF_L, MF_R,7_R	6_R,ML_R	7_L	0	0
MADA	CM_L,CM_R,SM_L,SM_R, ML_R,MF_R,7_L	6_L,6_R,MF_L	ML_L	7_R	0
MAMA	CM_L,6_R,ML_L,MF_R	CM_R,6_L,SM_L, SM_R,ML_R,MF_L	7_L	7_R	0
	SCI				
	Cluster 1	Cluster 2	Cluster 3	Cluster 4	Cluster 5
BARO	CM_L,CM_R,6_L,6_R, SM_L,ML_R,MF_L,MF_R	SM_R,ML_L	7_L	7_R	0
IRIO	CM_L,CM_R,6_L,SM_L, SM_R,ML_L,MF_L,MF_R	6_R	ML_R	7_L	7_R
MASI	CM_L,CM_R,6_L,SM_L, SM_R,ML_R,MF_R,7_L	6_R	ML_L	MF_L	7_R
POAL	CM_L,CM_R,SM_L, SM_R,MF_L	6_L,ML_R,MF_R	7_L,7_R	6_R	ML_L
TRDA	CM_L,CM_R,SM_L,SM_R, MF_L,MF_R,7_L,7_R	6_R,ML_R	6_L	ML_L	0

motor areas CM_L and CM_R, the SM_L and SM_R and the MF_L and MF_R, the second cluster does not present a common set of ROIs across the experimental subjects neither in the CTRL or the SCI group.

4. Discussion

The evaluation of the estimated cortical networks was addressed by means of a set of measures typical of complex network analysis [Boccaletti *et al.*, 2006; Micheloyannis *et al.*, 2006; Stam & Reijneveld, 2007; Hilgetag *et al.*, 2000]. We have first computed global (E_g) and local efficiency (E_l), two measures that allow characterizing the organization of the functional flows in both the inspected populations [De Vico Fallani *et al.*, 2007b]. The results indicate that spinal cord injuries significantly ($p < 0.05$) affect only the local properties of the functional architecture of the cortical network in the movement preparation. The global property of long-range integration between the ROIs within the network did not differ significantly ($p > 0.05$) from the healthy behavior. The higher average value of local efficiency in the SCI group suggests a larger level of the internal organization and a higher tendency to form modules. In particular, this difference can be observed in the two frequency bands Alpha (7–12 Hz) and Beta (13–29 Hz) that are already known for their involvement in electrophysiological phenomena related to the preparation and to the execution of limbs movements [Pfurtscheller & Lopes da Silva, 1999]. Although the efficiency indexes describe the network topology concisely, they are not able to give information about the number of modules and their composition within the network. For this reason, the detection of community structures was addressed by means of the Markov Clustering (MCl) algorithm [Vandongen, 2000; Enright *et al.*, 2002]. The same method has already been used successfully to detect clusters in sequence similarity networks [Enright *et al.*, 2002] and in configuration space networks derived from free-energy landscapes [Gfeller *et al.*, 2007]. The obtained results reveal a different average number of clusters for the functional networks of the

spinal cord injured patients and the control subjects in both the main spectral contents. In particular, in the Alpha band the SCI network presents an average number of modules equal to five, while the CTRL network appears to be divided into three groups. This outcome is in accordance with the significant ($p < 0.05$) higher level of local-efficiency found in the functional networks of the SCI patients with respect to the control subjects. A high E_l value reflects a high clustering index C and therefore a high density of network communities. The cortical areas of the control subjects do not present a clear partitioning in different modules. They rather appear to belong to a unique community, meaning that they are all involved, in the same way, in the exchange of information during the movement preparation. The analysis of the functional communities within the networks obtained for the spinal cord patients revealed a higher tendency to form separate clusters. The premotor areas (Brodmann 6_L and 6_R), the associative regions (Brodmann 7_L and 7_R) and the right primary motor area of the foot (MF_R) break away from the large module that was found in the networks of the CTRL group. In particular, the area MF_R and the region 6_L belong to the same cluster in at least three experimental patients. This result reveals the necessity of the SCI networks to hold a more efficient communication between these frontal premotor and primary motor structures, which are already known to be active during the successful execution of a simple movement [Ohara *et al.*, 2001]. In the Beta band, the average number of identified clusters in the SCI networks and in the CTRL networks is less different. Moreover, the ROIs that appeared to belong to different clusters in the Alpha band are in this case functionally tied in the same community. In summary, while in the Alpha band the control group mostly presented a unique large cluster; the spinal cord injured patients mainly exhibited two clusters. These two largest communities are mainly composed of the cingulate motor areas with the supplementary motor areas and of the premotor areas with the right primary motor area of the foot. This functional separation is thought to be responsible for the highest level of internal organization in the estimated networks and strengthens the hypothesis of a compensative mechanism due to the partial alteration in the primary motor areas because of the effects of the spinal cord injury [De Vico Fallani *et al.*, 2007a].

Acknowledgments

The present study was performed with the support of the COST EU project NEUROMATH (BMB 0601), of the Minister for Foreign Affairs, Division for the Scientific and Technologic Development, in the framework of a bilateral project between Italy and China (Tsinghua University). This paper only reflects the author' views and funding agencies are not liable for any use that may be made of the information contained herein.

Notes

In the current work, all the estimated functional networks are treated as unweighted and directed graphs. They all have the same number of connections representing the 25% (for the community structure analysis) and the 30% (for the efficiency indexes analysis) most powerful links within the network. These particular values belonged to an interval of thresholds (from 0.1 to 0.5), for which results remained significantly stable [De Vico Fallani *et al.*, 2007a].

References

Achard, S. & Bullmore, E. [2007] "Efficiency and cost of economical brain functional networks," *PloS Comp. Biol.* **3**, 17.

Astolfi, L., Cincotti, F., Mattia, D., Babiloni, C., Carducci, F., Basilisco, A., Rossini, P. M., Salinari, S., Ding, L., Ni, Y., He, B. & Babiloni, F. [2005] "Assessing cortical functional connectivity by linear inverse estimation and directed transfer function: Simulations and application to real data," *Clin. Neurophysiol.* **116**, 920–932.

Astolfi, L., Cincotti, F., Mattia, D., Marciani, M. G., Baccal, L., De Vico Fallani, F., Salinari, S., Ursino, M., Zavaglia, M., Ding, L., Edgar, J. C., Miller, G. A., He, B. & Babiloni, F. [2007] "A comparison of different cortical connectivity estimators for high resolution EEG recordings," *Human Brain Mapp.* **28**, 143–157.

Babiloni, F., Cincotti, F., Babiloni, C., Carducci, F., Basilisco, A., Rossini, P. M., Mattia, D., Astolfi, L., Ding, L., Ni, Y., Cheng, K., Christine, K., Sweeney, J. & He, B. [2005] "Estimation of the cortical functional connectivity with the multimodal integration of high resolution EEG and fMRI data by Directed Transfer Function," *Neuroimage* **24**, 118–131.

Bartolomei, F., Bosma, I., Klein, M., Baayen, J. C., Reijneveld, J. C., Postma, T. J., Heimans, J. J., van Dijk,

B. W., de Munck, J. C., de Jongh, A., Cover, K. S. & Stam, C. J. [2006] "Disturbed functional connectivity in brain tumour patients: Evaluation by graph analysis of synchronization matrices," *Clin. Neurophysiol.* **117**, 2039–2049.

Bassett, D. S., Meyer-Linderberg, A., Achard, S., Duke, T. H. & Bullmore, E. [2006] "Adaptive reconfiguration of fractal small-world human brain functional networks," *Proc. Natl. Acad. Sci.* **103**, 19518–19523.

Boccaletti, S., Latora, V., Moreno, Y., Chavez, M. & Hwang, D. U. [2006] "Complex networks: Structure and dynamics," *Phys. Rep.* **424**, 175-308.

David, O., Cosmelli, D. & Friston, K. J. [2004] "Evaluation of different measures of functional connectivity using a neural mass model," *Neuroimage* **21**, 659–673.

De Vico Fallani, F., Astolfi, L., Cincotti, F., Mattia, D., Marciani, M. G., Salinari, S., Kurths, J., Gao, S., Cichocki, A., Colosimo, A. & Babiloni, F. [2007a] "Cortical functional connectivity networks in normal and spinal cord injured patients: Evaluation by graph analysis," *Human Brain Mapp.* **28**, 1334–1346.

De Vico Fallani, F., Astolfi, L., Cincotti, F., Mattia, D., Tocci, A., Marciani, M. G., Colosimo, A., Salinari, S., Gao, S., Cichocki, A. & Babiloni, F. [2007b] "Extracting information from cortical connectivity patterns estimated from high resolution EEG recordings: A theoretical graph approach," *Brain Topogr.* **19**, 125–136.

Enright, A. J., Van Dongen, S. & Ouzounis, C. A., [2002] "An efficient algorithm for large-scale detection of protein families," *Nucl. Acids Res.* **30**, 1575–1584.

Gfeller, D., De Los Rios, P., Caflisch, A. & Rao, F. [2007] "From the cover: Complex network analysis of free-energy landscapes," *Procl. Natl. Acad. Sci.* **104**, 1817–1822.

Eguiluz, V. M., Chialvo, D. R., Cecchi, G. A., Baliki, M. & Apkarian, A. V. [2005] "Scale-free brain functional networks," *Phys. Rev. Lett.* **94**, 018102–018106.

Flake, G. W., Lawrence, S., Lee Giles, C. & Coetzee, F. M. [2002] "Self-organization and identification of web communities," *IEEE Comput.* **35**, 66–71.

Girvan, M. & Newman, M. E. J. [2002] "Community structure in social and biological networks," *Proc. Natl. Acad. Sci.* **99**, 7821–7826.

Granger, C. W. J. [1969] "Investigating causal relations by econometric models and cross-spectral methods," *Econometrica* **37**, 424–438.

Grave de Peralta Menendez, R. & Gonzalez Andino, S. L. [1999] "Distributed source models: Standard solutions and new developments," in *Analysis of Neurophysiological Brain Functioning*, ed. Uhl, C. (Springer-Verlag, Berlin), pp. 176–201.

Grigorov, M. G. [2005] "Global properties of biological networks," *DDT* **10**, 365–372.

Guimerà, R. & Amaral, L. A. N. [2005] "Functional cartography of complex metabolic networks," *Nature* **433**, 895–900.

Harary, F. & Palmer, E. M. [1973] *Graphical Enumeration* (Academic Press, NY), p. 124.

Hilgetag, C. C., Burns, G. A. P. C., O'Neill, M. A., Scannell, J. W. & Young, M. P. [2000] "Anatomical connectivity defines the organization of clusters of cortical areas in the macaque monkey and the cat," *Philos. Trans. R. Soc. Lond. B. Biol. Sci.* **355**, 91–110.

Horwitz, B. [2003] "The elusive concept of brain connectivity," *Neuroimage* **19**, 466–470.

Kaminski, M., Ding, M., Truccolo, W. A. & Bressler, S. [2001] "Evaluating causal relations in neural systems: Granger causality, directed transfer function and statistical assessment of significance," *Biol. Cybern.* **85**, 145–157.

Krause, A. E., Frank, K. A., Mason, D. M., Ulanowicz, R. E. & Taylor, W. W. [2003] "Compartments exposed in food-web structure," *Nature* **426**, 282–285.

Lago-Fernandez, L. F., Huerta, R., Corbacho, F. & Siguenza, J. A. [2000] "Fast response and temporal coherent oscillations in small-world networks," *Phys. Rev. Lett.* **84**, 2758–2761.

Latora, V. & Marchiori, M. [2001] "Efficient behavior of small-world networks," *Phys. Rev. Lett.* **87**, 198701.

Latora, V. & Marchiori, M. [2003] "Economic small-world behavior in weighted networks," *Eur. Phys. J. B.* **32**, 249–263.

Latora, V. & Marchiori, M. [2005] "Vulnerability and protection of infrastructure networks," *Phys. Rev. E* **71**, 015103R.

Latora, V. & Marchiori, M. [2007] "A measure of centrality based on network efficiency," *New J. Phys.* **9**, 188.

Lee, L., Harrison, L. M. & Mechelli, A. [2003] "The functional brain connectivity workshop: Report and commentary," *Neuroimage* **19**, 457–465.

Lusseau, D. & Newman, M. E. J. [2004] "Identifying the role that animals play in their social networks," *Proc. Roy. Soc. London B* **271**, S477–S481.

Micheloyannis, S., Pachou, E., Stam, C. J., Vourkas, M., Erimaki, S. & Tsirka, V. [2006] "Using graph theoretical analysis of multi channel EEG to evaluate the neural efficiency hypothesis," *Neurosci. Lett.* **402**, 273–277.

Milgram, S. [1967] "The small world problem," *Psychol. Today* **1**, 60–67.

Newman, M. E. J. [2003] "The structure and function of complex networks," *SIAM Rev.* **45**, 167–256.

Ohara, S., Mima, T., Baba, K., Ikeda, A., Kunieda, T., Matsumoto, R., Yamamoto, J., Matsuhashi, M., Nagamine, T., Hirasawa, K., Hon, T., Mihara, T., Hashimoto, N., Salenius, S. & Shibasaki, H. [2001] "Increased synchronization of cortical oscillatory activities between human supplementary motor and

primary sensorimotor areas during voluntary movements," *J. Neurosci.* **21**, 9377–9386.

Palla, G., Derenyi, I., Farkas, I. & Vicsek, T. [2005] "Uncovering the overlapping community structure of complex networks in nature and society," *Nature* **435**, 814–818.

Pfurtscheller, G. & Lopes da Silva, F. H. [1999] "Event-related EEG/MEG synchronization and desynchronization: Basic principles," *Clin. Neurophysiol.* **110**, 1842–1857.

Pimm, S. L. [1979] "The structure of food webs," *Theor. Popul. Biol.* **16**, 144–158.

Salvador, R., Suckling, J., Coleman, M. R., Pickard, J. D., Menon, D. & Bullmore, E. [2005] "Neurophysiological architecture of functional magnetic resonance images of human brain," *Cereb Cort.* **15**, 1332–1342.

Sporns, O., Tononi, G. & Edelman, G. E. [2000] "Connectivity and complexity: The relationship between neuroanatomy and brain dynamics," *Neural Netw.* **13**, 909–922.

Sporns, O. [2002] "Graph theory methods for the analysis of neural connectivity patterns," in *Neuroscience Databases, A Practical Guide*, ed. Kötter, R., pp. 171–185.

Sporns, O., Chialvo, D. R., Kaiser, M. & Hilgetag, C. C. [2004] "Organization, development and function of complex brain networks," *Trends Cogn. Sci.* **8**, 418–425.

Sporns, O. & Zwi, J. D. [2004] "The small world of the cerebral cortex," *Neuroinformatics* **2**, 145–162.

Stam, C. J. [2004] "Functional connectivity patterns of human magnetoencephalographic recordings: A 'small-world' network?" *Neurosci. Lett.* **355**, 25–28.

Stam, C. J., Jones, B. F., Manshanden, I., van Cappellen van Walsum, A. M., Montez, T., Verbunt, J. P., de Munck, J.C., van Dijk, B.W., Berendse, H.W. & Scheltens, P. [2006a] "Magnetoencephalographic evaluation of resting-state functional connectivity in Alzheimer's disease," *Neuroimage* **32**, 1335–1344.

Stam, C. J., Jones, B. F., Nolte, G., Breakspear, M. & Scheltens, P. [2006b] "Small-world networks and functional connectivity in Alzheimer's disease," *Cereb. Cortex* **17**, 92–99.

Stam, C. J. & Reijneveld, J. C. [2007] "Graph theoretical analysis of complex networks in the brain," *Nonlin. Biomed. Phys.* **1**, 3 epub.

Strogatz, S. H. [2001] "Exploring complex networks," *Nature* **410**, 268–276.

Tononi, G., Sporns, O. & Edelman, G. M. [1994] "A measure for brain complexity: Relating functional segregation and integration in the nervous system," *Proc. Natl. Acad. Sci.* **91**, 5033–5037.

Van Dongen, S. [2000] *Graph Clustering by Flow Simulation*, PhD thesis, University of Utrecht.

Watts, D. J. & Strogatz, S. H. [1998] "Collective dynamics of 'small-world' networks," *Nature* **393**, 440–442.